Time-Resolved L-Shell Absorption Spectroscopy: A Direct Measurement of Density and Temperature in a Germanium Laser-Produced Plasma

J. Bruneau,[1] C. Chenais-Popovics,[2] D. Desenne,[1] J.-C. Gauthier,[2] J.-P. Geindre,[2] M. Klapisch,[3] J.-P. Le Breton,[1] M. Louis-Jacquet,[1] D. Naccache,[1] and J.-P. Perrine[1]

[1]*Centre d'Etudes de Limeil-Valenton, 94195 Villeneuve-St-Georges, France*

[2]*Laboratoire de Physique des Milieux Ionisés, Ecole Polytechnique, 91128 Palaiseau, France*

[3]*Lawrence Livermore National Laboratory, Livermore, California*

(Received 24 May 1990)

L-shell absorption of germanium transitions has been exploited for the first time to diagnose the low-temperature, high-density region of multilayered targets irradiated by 0.35-μm laser light at irradiances around 10^{14} W/cm^2. A detailed atomic physics package has been used to relate the observed absorption wavelengths to the ionic distribution from Ge VII to Ge XX and to the electron plasma parameters. Results show time-dependent temperature variations following closely the driving laser pulse shape in agreement with hydrocode simulations.

PACS numbers: 52.50.Jm, 52.25.Nr

In the past few years, absorption x-ray spectroscopy has been shown to be an interesting diagnostic tool of high-density, low-temperature plasmas.[1-5] $K\alpha$ transitions in the 5–10-Å wavelength range have been used to probe the electron-temperature gradient in plasmas of low-Z elements.[6,7] In the inertial-fusion community, there has been a recent surge of interest in the diagnostic problem of temperature and areal density ρr in much-higher-Z materials, motivated by the use of high-mass pushers in direct- or indirect-drive capsule design.[8] In this case, it is no longer possible to use $K\alpha$ lines. This is due to the fact that the corresponding absorbing ions must have a $2p$ vacancy for K-shell absorption to occur. In the $Z \approx 30$ range, H-like to F-like ions are populated at electron temperatures which are by far too high with respect to the desirable diagnostic temperature range of 20–200 eV. L-shell absorption should be more appropriate for that purpose.

In this Letter we present the first experimental study of L-shell absorption in a laser-produced plasma. We have used germanium ($Z=32$) ions pertaining to the Al-like to Co-like isoelectronic series. We have been able to directly follow the time evolution of the electron temperature during the driving laser pulse. This has been done by measuring the wavelength of the absorption feature as a function of time. We have determined the distribution of ionic stages in the plasma from a detailed atomic physics package including the relevant electronic configurations. Results have been compared to the predictions of a 1D hydrocode incorporating photon energy transport physics.

Basically, the principle of the experiment is similar to our previous measurements of K-shell absorption in aluminum and chlorine.[6] The targets consist in thin foils having two or three layers. The first layer, directly irradiated by the laser, is made of praseodymium (Pr, $Z=59$). Sub-keV Pr x rays create a radiative wave towards the inside of the target where their energy is deposited. Scaling laws of the radiative-wave parameters[9] show that electron temperatures of the order of 100 eV can be achieved for materials of $Z \approx 30$. keV Pr x rays are used as a backlighter source. Praseodymium has been chosen because its $3l$-$4l'$ and $3l$-$5l'$ unresolved transition array emissions from V-like to Ni-like ions provide a relatively smooth spectrum in the 9–11-Å range where Ge VII to Ge XX ions absorb. The thickness of the Pr layer (0.6 μm) has been determined from a compromise between the need for incomplete laser ablation and maximum x-ray conversion efficiency at the nominal irradiance of 10^{14} W/cm^2. The second layer is optional and is made of silicon. It acts as a variable thickness spacer (0–2 μm) allowing us to vary the position of the Ge layer along the electron-temperature gradient. Silicon has been chosen for its good transparency to x rays around 1.2 keV and because it shows a hydrodynamic behavior which is not too different from that of Ge. Finally, the 0.5-μm Ge layer thickness was inferred from previous experiments[6] in aluminum to ensure a homogeneous electron temperature in the absorbing layer.

The experiments were performed at the Centre d'Etudes de Limeil-Valenton using two beams of the Octal Nd:glass laser facility. Random-phase plates designed for 0.35 μm wavelength were used to produce a smooth laser energy distribution (no more than 20% irregularities) of Gaussian shape with 200 μm FWHM. The laser delivered 60 J in a pulse of 1 ns FWHM providing irradiances up to 1.5×10^{14} W/cm^2 on target. The temporal shape of the laser was almost flat during 800 ps with rising and falling edges of about 200 ps. At the rear side of the target, spectra were recorded by two 400-mm-diam curved thallium acid phthalate crystal spectrographs symmetrically set at angles of 37° with respect to the target-plane normal. One of them used Kodak SB2 x-ray film as a detector providing a time-integrated spectrum with a rocking-curve–limited resolution of 600. The other was equipped with a streak cam-

era with 30-ps time resolution and with a spectral resolution of 150. Intensity versus density calibration of the film has been previously determined[10] and checked by using appropriate x-ray wedges. The plasma was also diagnosed by a flat thallium acid phthalate crystal spectrograph which viewed the front side of the target. Laser spot sizes were measured by a pinhole camera filtered for x rays in the keV range.

Integrated spectra obtained with a 0.6-μm Pr layer deposited on 2-μm plastic (CH) were used as a reference to give a determination of the backlighter source intensity since CH is optically thin to keV radiation. Subtracting the reference spectra from the spectra obtained with a 0.6-μm Pr layer deposited on 0.5 μm of Ge and with a 0.6-μm Pr layer on 1.9 μm of Si and 0.5 μm of Ge allows us to calculate the optical depth of the Ge layer without and with the silicon spacer. Results are shown in Figs. 1(a) and 1(b), respectively. Qualitatively, the absorption structure shifts to longer wavelengths (lower energies) and is narrower in Fig. 1(b). Since the absorption wavelength of a given ion increases when the charge decreases, this indicates that lower electron temperatures are probed by the Ge layer when a silicon spacer is present. In Fig. 1(a), the $2p$-$3d$ absorption band lies between 9.1 and 9.7 Å corresponding to Al-like to Ar-like germanium ions. The barely visible feature at wavelengths below 8.4 Å can be attributed to the $2p$-$4d$ absorption band from our theoretical calculations. In Fig. 1(b), the $2p$-$3d$ absorption band lies between 9.4 and 10.2 Å and is produced by S-like to Ti-like ions. Around 7 Å the $1s$-$2p$ absorbing lines of Si provide information on the spectral resolution. Based on our previous study of $K\alpha$ absorption,[6,7] we deduce from the relative intensities of the Si absorption lines an electron temperature of the order of 90 eV in the silicon layer.

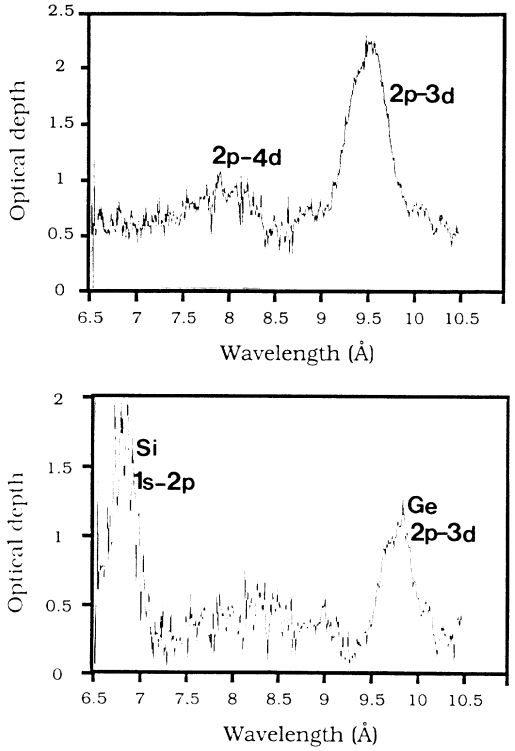

FIG. 1. Optical depth as a function of wavelength. (a) 0.6-μm-Pr/0.5-μm-Ge and (b) 0.6-μm-Pr/1.9-μm-Si/0.5-μm-Ge. Laser energies are around 80 J; laser wavelength is 0.35 μm.

Figure 2 shows a record of the spectrum taken by the time-resolving rear spectrograph during the same shot as in Fig. 1(a). A shift to higher energies of the central wavelength of the $2p$-$3d$ Ge absorption band as a function of time can be clearly seen. The greater shifts coincide in time with the maximum emission of the Pr layer which occurs during the flat portion of the laser pulse. During this phase the absorption spectrum is very close to the integrated one of Fig. 1(a). Furthermore, the time variation of the shift follows the temporal shape of the laser pulse, indicating that the temperatures in the Ge and Pr layers are closely related.

In order to interpret these experiments, we have first determined the electron temperature and density from hydrodynamical calculations and, second, we have simulated the measured spectra by using the previously determined plasma parameters as input to a detailed atomic physics code.

The hydrodynamic simulations use a one-dimensional hydrocode[11] (XRAD) including photon transport by a multigroup radiative transfer method. Emission coefficients and opacities for Pr and Ge have been calculated using a simple, non-local-thermodynamic-equilibrium (LTE), average atom model[11] neglecting l splitting. This code is very similar to the hydrocode MULTI[12,13] and its usefulness in radiation energetics has been demonstrated.[14] Figure 3 gives the evolution of the electron temperature and density inside the Ge layer calculated by XRAD under the experimental conditions of Fig.

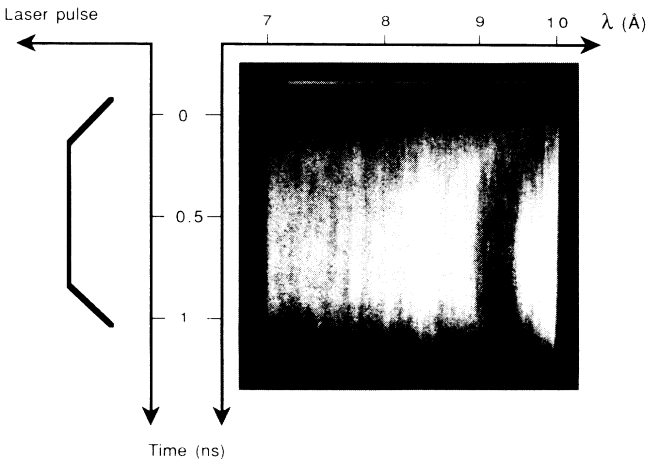

FIG. 2. Streak photograph of the time-resolved rear spectra of the shot in Fig. 1(a) showing Ge absorption wavelength following closely the shape of the laser pulse.

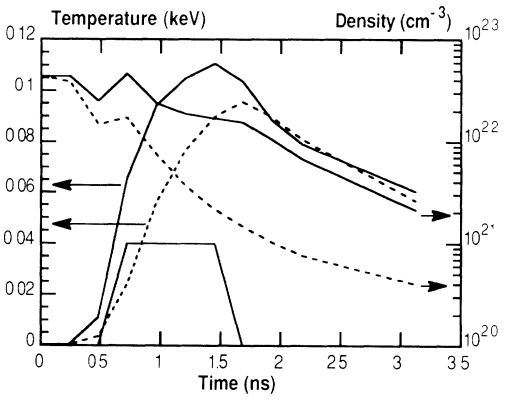

FIG. 3. Electron temperature (left) and density (right) as a function of time calculated by XRAD with 10^{14} W/cm^2 and 0.35-μm laser irradiance and wavelength. Solid line: results for the cell adjacent to the Pr layer. Dashed line: results for the cell located at the rear of the Ge layer. The laser pulse shape is shown at the bottom.

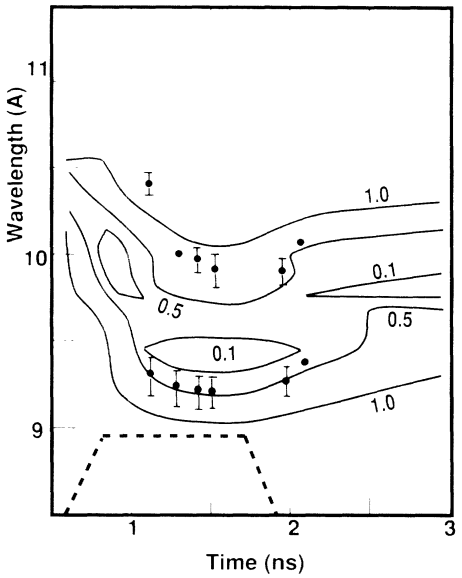

FIG. 4. Wavelength of the low- and high-energy limits of the $2p$-$3d$ Ge absorption band giving 50% transmission as a function of time. Squares: experimental points. The isocontours have been calculated by XRAD and the atomic physics code. The error bars show the uncertainties in the backlighter emission.

1(a). The front temperature in the Ge layer, i.e., the region closest to the Pr layer (solid line), is of the order of 100 eV for a time period of about 800 ps slightly shifted with respect to the flat portion of the laser pulse. The rear temperature in the Ge layer (dashed line) is 20 eV lower during the laser pulse and reaches values comparable to the front temperature at times greater than 2 ns. Shock-heating and thermal-conduction effects can be safely ruled out as explaining such a shallow (from 100 to 80 eV) temperature gradient. From the simulations, shock heating was found to be smaller than 10 eV under our low-irradiance conditions. Using the hydrocode with and without radiative transfer, we have shown that thermal conduction gives rise to steeper temperature gradients and lower temperature values in the Pr layer during the laser pulse. These results indicate that radiative heating[9] of the Ge layer occurs through laser light conversion to x rays in the Pr layer followed by x-ray energy deposition in the Ge layer.

To evaluate the degree of confidence in our radiation modeling we have compared the experimental absolute time-integrated emission intensity at the front of the target, which is essentially due to the Pr layer, with the calculated front spectrum in the 1200–1500-eV range. A good agreement, within a factor of 2, was found between experiment and theory. This is particularly gratifying since first, the uncertainties in the crystal-film-geometry combination are quite large in this kind of experiment and, second, the atomic physics is treated rather roughly in the hydrocode.

A detailed atomic physics code was used as a postprocessor to the hydrocode simulations to calculate the shape of the absorption spectrum. The wavelengths and the radiative rates of Ge ions from Al-like to Co-like ions have been calculated both with the RELAC code[15] and with multiconfiguration Dirac-Fock programs.[16] As the total number of levels of an ion with partially filled shells can be very large, we have restricted our calculations to the ground $2p^6 3s^l ep^{l'} 3d^{l''}$ and excited $2p^5 3s^l 3p^{l'} 3d^{l''+1}$ configurations of Al-like ($l'=1$, $l''=0$) to Co-like ($l'=6$, $l''=9$) ions. As an example, for the Ge XI ion, $2p$-$3d$ absorption involves more than 3000 lines. Calculations of low-lying level populations have been obtained by a LTE model. The validity of LTE was checked in our density and temperature range (around 10^{22} cm^{-3} and 100 eV) by using a stationary collisional-radiative model incorporating ten excited levels by ion and hydrogenic collisional and radiative rates.

We have plotted in Fig. 4 the measured time variation of the low- and high-wavelength limits of the $2p$-$3d$ absorption feature corresponding to 50% transmission. The calculated transmission at the 100%, 50%, and 10% levels, taking into account the measured instrumental resolution, has also been plotted for comparison. The experimental data set covers only a 1-ns time interval which corresponds to the duration of the Pr emission and of the laser pulse. As no absolute timing was available from the experiment, the maximum of the Pr emission was used as a reference. A good agreement between theory and experiment can be seen for the high-energy (low-wavelength) side of the absorption feature while a small discrepancy exists on the low-energy side. This is partly due to the neglect of the partially filled configurations of the type $2p^6 3s^{l-m} 3p^{l'-m'} 3d^{l''+m+m'}$ when additional vacancies are opened in the $3s$ and $3p$ shells. Actually, these configurations give a low-energy wing to the rel-

evant $2p$-$3d$ absorption lines. In addition, deviations from LTE cannot be ruled out at the rear side of the target (see Fig. 3). Non-LTE effects generally give an average charge lower than LTE which results in a global shift of the absorption feature towards longer wavelengths.

In summary, we have demonstrated for the first time the usefulness of $2p$-$3d$ absorption spectroscopy for plasma diagnostics in medium-Z materials. Comparison of the time variation of the experimental absorption wavelengths with simulations involving atomic physics and hydrocode calculations shows a noteworthy agreement and allows the determination of the distribution of ionic stages in the plasma and thus the electron density and temperature. Work is actually in progress using the unresolved-transition-array (UTA) formalism including spin-orbit splitting[17,18] to evaluate the effect of neglecting partially filled configurations in the simulation of the spectra and to give an extension of the present technique to much-higher-Z materials.

We would like to thank Y. Gord, J. Kobus, J.-L. Larcade, M. Rabec le Gloahec, A. Steib, B. Pupille, and J. Turberville for the help on the Heliotrope target chamber, the Octal laser team, and the very efficient and skillful work of M. Bellingard and M. Millerioux for the target preparation. Fruitful discussions with J. Bauche and C. Bauche-Arnoult were also very helpful during the completion of that work. Laboratoire de Physique des Milieux Ionisés is a unité associée au CNRS.

[1]A. Hauer, R. W. Cowan, B. Yaakobi, O. Barnouin, and R. Epstein, Phys. Rev. A **34**, 411 (1986).

[2]D. K. Bradley, J. D. Hares, and J. D. Kilkenny, Rutherford Appleton Laboratory, Annual Report No. RL-83-043, 1983 (unpublished), p. 5.4.

[3]C. Chenais-Popovics, C. Fievet, J. P. Geindre, J. C. Gauthier, J. F. Wyart, and E. Luc-Koenig, Proc. SPIE Int. Soc. Opt. Eng. **831**, 30 (1987).

[4]P. Audebert, D. K. Bradley, M. C. Richardson, R. Epstein, P. A. Jaanimagi, O. Barnouin, J. Delettrez, B. Yaakobi, F. J. Marshall, and B. L. Henke, Proc. SPIE Int. Soc. Opt. Eng. **831**, 9 (1987).

[5]E. Jannitti, P. Nicolosi, and G. Tondello, Physica (Amsterdam) **124C**, 139 (1984); J. Phys. (Paris), **41**, C1-71 (1988).

[6]C. Chenais-Popovics, C. Fievet, J. P. Geindre, J. C. Gauthier, E. Luc-Koenig, J. F. Wyart, H. Pépin, and M. Chaker, Phys. Rev. A **40**, 3194 (1989).

[7]C. Chenais-Popovics, C. Fievet, J. P. Geindre, J. C. Gauthier, and I. Matsushima, in Proceedings of the Twentieth European Conference on Laser Interaction with Matter, Schliersee, 1990 (unpublished).

[8]E. Storm, in *Laser Interaction with Matter,* edited by G. Velarde, E. Minguez, and J. M. Perlado (World Scientific, Singapore, 1989), p. 85.

[9]R. Sigel, K. Eidmann, F. Lavarenne, and R. F. Schmalz, Phys. Fluids B **2**, 199 (1990); **2**, 208 (1990).

[10]H. Dumont and P. Troussel (to be published).

[11]J. P. Geindre and J. C. Gauthier, Laboratoire PMI, Ecole Polytechnique Reports No. 1971 and No. 1974, 1988 (unpublished), available upon request from the authors.

[12]R. Ramis, R. Schmalz, and J. Meyer-ter-Vehn, Comput. Phys. Commun. **49**, 475 (1988).

[13]K. Eidmann, in *Inertial Confinement Fusion,* Proceedings of the International School of Plasma Physics "Piero Caldirola," edited by A. Caruso and E. Sindoni (Commission of the European Communities, Brussels, 1988), EUR11930 EN, p. 65.

[14]I. Toubhans, R. Fabbro, J. C. Gauthier, H. Pépin, and A. Chaker, Proc. SPIE Int. Soc. Opt. Eng. **1140**, 358 (1989).

[15]E. Luc-Koenig, Physica (Utrecht) **62**, 393 (1972); E. Luc-Koenig, M. Klapisch, and A. Bar-Shalom, computer code RELAC.

[16]J. Bruneau, J. Phys. B **17**, 3009 (1984).

[17]C. Bauche-Arnoult, J. Bauche, and M. Klapisch, Phys. Rev. A **31**, 2248 (1985).

[18]J. Bauche, C. Bauche-Arnoult, and M. Klapisch, Adv. At. Mol. Phys. **23**, 131 (1987).

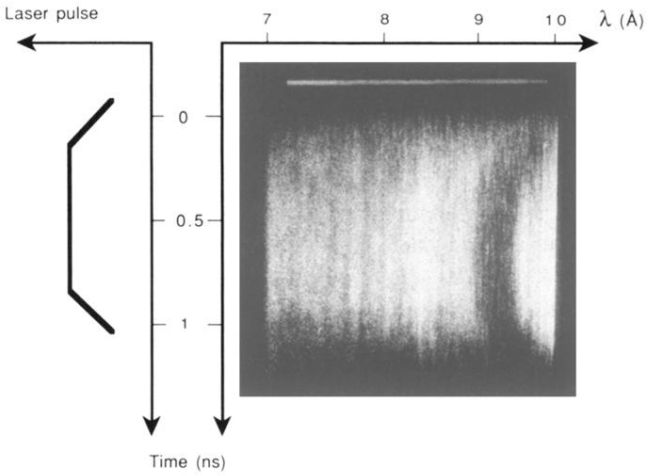

FIG. 2. Streak photograph of the time-resolved rear spectra of the shot in Fig. 1(a) showing Ge absorption wavelength following closely the shape of the laser pulse.